

REPORT



Toward *in vitro*-to-*in vivo* translation of monoclonal antibody pharmacokinetics: Application of a neonatal Fc receptor-mediated transcytosis assay to understand the interplaying clearance mechanisms

Claudia A. Castro Jaramillo^{a,*}, Sara Belli^{a,*}, Anne-Christine Cascais^a, Sherri Dudal^{ib}, Martin R. Edelmann^a, Markus Haak^a, Marie-Elise Brun^{ib}, Michael B. Otteneder^a, Mohammed Ullah^a, Christoph Funk^a, Franz Schuler^a, and Silke Simon^a

^aRoche Pharmaceutical Research and Early Development, Roche Innovation Center, Basel, Switzerland; ^bUCB Celltech, Slough, UK

ABSTRACT

Monoclonal antibodies (mAbs) are a rapidly growing drug class for which great efforts have been made to optimize certain molecular features to achieve the desired pharmacokinetic (PK) properties. One approach is to engineer the interactions of the mAb with the neonatal Fc receptor (FcRn) by introducing specific amino acid sequence mutations, and to assess their effect on the PK profile with *in vivo* studies. Indeed, FcRn protects mAbs from intracellular degradation, thereby prolongs antibody circulation time in plasma and modulates its systemic clearance. To allow more efficient and focused mAb optimization, *in vitro* input that helps to identify and quantitatively predict the contribution of different processes driving non-target mediated mAb clearance *in vivo* and supporting translational PK modeling activities is essential. With this aim, we evaluated the applicability and *in vivo*-relevance of an *in vitro* cellular FcRn-mediated transcytosis assay to explain the PK behavior of 25 mAbs in rat or monkey. The assay was able to capture species-specific differences in IgG-FcRn interactions and overall correctly ranked Fc mutants according to their *in vivo* clearance. However, it could not explain the PK behavior of all tested IgGs, indicating that mAb disposition *in vivo* is a complex interplay of additional processes besides the FcRn interaction. Overall, the transcytosis assay was considered suitable to rank mAb candidates for their FcRn-mediated clearance component before extensive *in vivo* testing, and represents a first step toward a multi-factorial *in vivo* clearance prediction approach based on *in vitro* data.

ARTICLE HISTORY

Received 27 January 2017
Revised 31 March 2017
Accepted 11 April 2017

KEYWORDS

Neonatal Fc receptor (FcRn); monoclonal antibody; clearance; *in vitro*-to-*in vivo* correlation; transcytosis; cellular assays; pharmacokinetics

Introduction

Monoclonal antibodies (mAbs) have developed into one of the fastest growing drug classes. Considering the competitive environment within the pharmaceutical sector and the demand for mAbs against new targets, novel discovery platforms and antibody engineering are rapidly evolving, allowing the generation of molecules with engineered variable mAb domains to decrease immunogenicity,¹ bispecific mAbs targeting more than one antigen with optimized affinity,² fragment antigen-binding (Fab) domains³ and fragment crystallizable (Fc)-fusion proteins.^{4,5} In addition, great efforts have been made to optimize mAb clearance *in vivo* by e.g., modulating the Fc interaction with the neonatal Fc receptor (FcRn)^{6,7} or by adapting mAb physicochemical properties to prevent increased unspecific cellular uptake *via* pinocytosis.^{8,9} To develop effective and safe biologic drugs with reduced efficacious dose and more convenient administration route/frequency, mAbs must have suitable pharmacokinetic (PK) properties. Thus, preclinical optimization and characterization of mAb PK/pharmacodynamics (PD) profile and its translation to human is an essential step in biologics drug discovery.¹⁰

The Fc region of immunoglobulin G (IgG)-based antibodies plays an important role in determining their *in vivo* PK profile. One major process is their pH-dependent binding to FcRn, for which the Fc region has strong affinity at pH 6.0, but weak affinity at pH 7.4. FcRn is located within endosomes in endothelial cells lining blood vessels and haematopoietic cells. In addition to IgG molecules, it interacts with serum albumin using a different binding site.¹¹ FcRn ligands (i.e., IgG and albumin) in circulation are taken up by cells *via* non-specific fluid-phase pinocytosis, followed by binding to FcRn in the acidic environment (pH ~6.0) of the endosome.^{12,13} This complexation protects the ligand from lysosomal degradation, enabling the ligand-FcRn complex to be recycled back to the cell surface. At pH 7.4, the “protected” ligand bound to FcRn is then released from the complex to the extracellular space. Thereby, FcRn maintains IgG and albumin homeostasis in human and animal serum, and transfers maternal IgGs from the mother to the fetus over the placental barrier.¹³

The effect of mAb-FcRn interactions on plasma systemic clearance of mAbs has been extensively studied in preclinical species and in man, using various mutant mAbs with abolished^{14,15} or enhanced^{16–18} FcRn affinity. These studies confirmed that the

interaction with FcRn strongly affects the PK properties of therapeutic mAbs. Therefore, its accurate *in vitro* assessment, with a readout suitable for the quantitative prediction of FcRn-mediated PK properties *in vivo*, would be of great help to support drug candidate optimization/selection and to ensure an appropriate PK profile according to the desired drug product profile, as well as to minimize animal testing early in discovery.¹⁹

Preclinical PK properties of biologic drug candidates are currently assessed *in vivo* mostly in mice and in non-human primates. The preclinical PK parameters are typically translated to human using allometric scaling,²⁰ with or without the inclusion of “target-mediated drug disposition” (TMDD), depending on the specific case and the availability of kinetic information on the target. For mAbs exhibiting TMDD, the PK profile is often described by a 2-compartmental model with linear and nonlinear elimination. Both the linear clearance (CL) and nonlinear CL (V_{max}) of mAbs are typically scaled allometrically, with the Michaelis-Menten constant (K_m) assumed to be equal in monkeys and humans based on similar *in vitro* target binding characteristics or identical target protein sequences.²¹ However, *in vitro* tools that help to quantitatively scale all the different processes contributing to mAb disposition *in vivo* from animals to human are currently not available.

A routinely used *in vitro* approach for the qualitative study of mAb-FcRn interaction is the surface plasmon resonance (SPR) technique, which allows affinity measurement of a mAb for the FcRn at different pH conditions.²² However, in certain cases, affinity-based physicochemical FcRn methodologies failed to correlate with the observed clearance *in vivo*.²³ These limitations are likely due to additional biochemical and biophysical properties of the mAbs, along with their FcRn affinity, that influence the *in vivo* PK, such as “unspecific”/charge-dependent binding characteristics of the mAbs during the cellular uptake process *via* pinocytosis, the pH-dependent dissociation of the FcRn-IgG complexes and the effect of TMDD at non-target saturating dose levels.²⁴ More recently, new methodology using an FcRn-coated affinity column was introduced by Schlothauer *et al.*,¹⁴ where mAb-receptor binding and release was measured in a pH-dependent fashion and was correlated with the *in vivo* half-life of 3 mAbs.

Due to the complexity of the FcRn-mediated mAb recycling phenomenon *in vivo*, comprising interactions of the antibody with the cell membrane, mAb uptake *via* fluid-phase pinocytosis, FcRn-mediated intracellular sorting/trafficking/salvage from lysosomal degradation and finally mAb release at the cell membrane, we aimed to evaluate an *in vitro* tool mimicking the entire IgG-FcRn-interaction cycle in living cells, which is a more physiologically-like system.

Previously, Tesar *et al.* and Prator *et al.* described the use of FcRn-transfected Madin-Darby Canine kidney (MDCK) cells to assess FcRn-mediated transcytosis of mAbs. They monitored the flux of IgGs and other Fc-containing molecules across a tight cell monolayer plated in a Transwell® system, using acidic pH in the donor compartment and neutral pH in the acceptor compartment. This pH gradient strongly reduced IgG recycling back into the donor chamber and at the same time enabled FcRn-mediated endocytotic cellular uptake, which altogether maximized unidirectional FcRn-mediated trafficking.^{25,26}

Here, we describe the application of this cellular assay for understanding the *in vivo* FcRn-mediated protection from lysosomal catabolism of chimeric, human and humanized mAbs. Even though IgG recycling *in vivo*, which takes place, for example, in vascular endothelial cells, and the transcytotic IgG movement are not identical processes, the transcytotic IgG trafficking *in vitro* under optimized conditions may be used as a surrogate for IgG recycling *in vivo*. Using this *in vitro* transcellular flux as primary assay readout, a selected set of mAbs was tested in rat or human FcRn-expressing MDCK cells to differentiate their properties and to quantitatively correlate the data with their *in vivo* clearance values in rats and cynomolgus monkeys. Such a systematic evaluation of the correlation between *in vitro* parameters (FcRn-mediated mAb flux) and *in vivo* clearance, referred to here as *in vitro*-to-*in vivo* correlation (IVIVC), has not been available until now, but is considered essential to understand the multi-factorial mAb clearance mechanism *in vivo* by applying *in vitro* methodologies.

Results

Assessment of FcRn-mediated transcytosis of antibodies in rat or human FcRn receptor over-expressing cells

According to the described previously methods by Tesar *et al.*²⁵ and Praetor *et al.*,²⁶ MDCK cells transfected with either rat or human FcRn were cultured as tight monolayers and the antibody transport assay was conducted in the presence of a pH gradient (donor/acceptor compartment buffer at pH 6.0/8.0) to maximize uni-directional IgG transcytotic transport. The incubation without a pH gradient (donor/acceptor compartment buffer at pH 8.0/8.0) should allow determination of “unspecific,” receptor-independent antibody uptake. We conducted initial confirmatory studies with a ³H-labeled humanized mAb bearing no mutations in the FcRn binding region (herein named as wildtype “Wt” IgG) and targeting an antigen absent in the cells used for this assay. FITC-labeled dextran (MW 150 kDa), which is restricted to paracellular permeability, was included as a marker of monolayer tightness under the applied assay conditions.

Fig. 1 displays the basolateral to apical transport or flux of this ³H-labeled Wt IgG across human and rat FcRn over-expressing

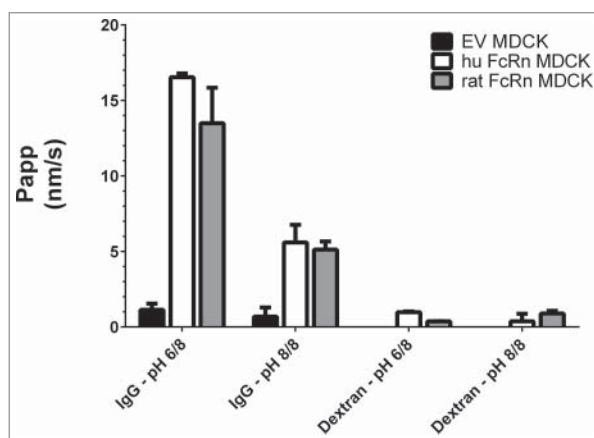


Figure 1. Basolateral to apical flux (P_{app}) of a ³H-IgG and FITC-dextran across rat and human FcRn over-expressing MDCK cells and EV cells. The highest P_{app} was observed in the cell line over-expressing FcRn and under pH 6.0/8.0, indicating a specific FcRn-mediated antibody transport. Data is shown as mean \pm SD; $n = 3$ (separate wells).

MDCK cells compared with “empty vector” (EV) transfected MDCK cells without FcRn as the functional negative control. The IgG flux at pH 6.0/8.0 across FcRn-transfected cells, displayed as apparent permeability “Papp” in nanometers per second (nm/s), ranged from 13 to 17 nm/s depending on the species, and was about 10-fold higher than across EV cells (1.1 nm/s), indicating a pronounced FcRn-mediated trafficking of the antibody. As expected, the antibody flux at pH 8.0/8.0 was significantly reduced due to the known weak mAb affinity for the FcRn receptor at pH 8.0, resulting in a flux of 5–6 nm/s, likely reflecting “unspecific” antibody uptake processes, such as pinocytosis, followed by FcRn-mediated transcellular trafficking. The control FITC-dextran showed negligible paracellular fluxes of ~1.0 nm/s, confirming the integrity of the cell layer under the applied assay conditions.

Species selectivity of rat and human FcRn-mediated IgG transcytosis

Rat, mouse, or chicken IgGs do not bind to the human FcRn, whereas IgGs from all mentioned species, apart from chicken, bind to rat FcRn.²⁷ To assess whether these species-selective IgG-FcRn interactions were captured in the studied assay, the flux of FITC-labeled mouse, rat, human and chicken IgGs was measured in both rat and human FcRn cell systems at pH 6.0/8.0 and pH 8.0/8.0. The chicken IgG served here as non-binding control. As depicted in Fig. 2, human FcRn over-expressing cells enabled a high flux of the human IgG at pH 6.0/8.0, and low fluxes of immunoglobulins from animal species. Rat FcRn over-expressing cells transported rat, mouse, and human IgG with a respectively increasing flux, which was in line with the higher affinity of human IgG for rat FcRn compared with rat or mouse IgGs.¹⁵

These data confirm the expected species-specific FcRn-traffic of IgGs in the rat and human FcRn cell systems. Further investigations addressing FcRn saturation by endogenous plasma IgGs, and their effect on therapeutic mAb flux *in vitro* are described in the supplemental material.

Transcytosis assay validation with ³H-labeled Fc-mutated IgGs

To validate the predictability of human and rat FcRn transcytosis assay for FcRn-driven *in vivo* CL of mAbs, the cellular flux

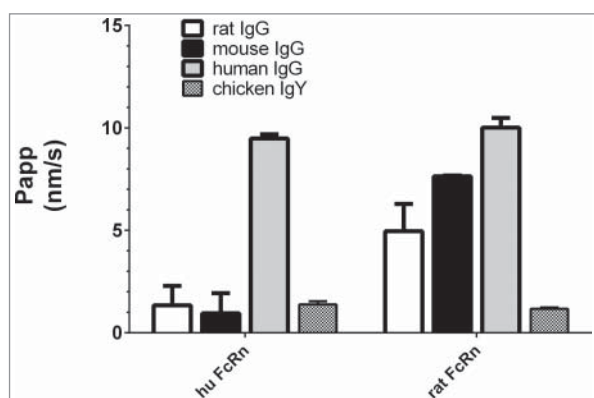


Figure 2. Basolateral to apical flux (Papp) of FITC-labeled rat, mouse, human IgGs and chicken IgY across human FcRn and rat FcRn MDCK cells with a pH gradient (6.0/8.0). The inability of rodent IgG to bind to human FcRn was confirmed. Data is shown as mean \pm SD; n = 3 (separate wells).

of 3 IgG1 molecules was evaluated. These mAbs contain an identical Fab part (anti-digoxigenin = <DIG>) but distinct Fc mutations known to modulate the FcRn affinity. IgG *Wildtype* (Wt) has unmodified FcRn binding ability (without mutation in the FcRn-binding region of the Fc part). In the IgG AAA (*Triple A mutant M252A/H310A/H435A*), 3 of the main amino acids associated with the Fc-FcRn interactions were replaced by alanine, abolishing the FcRn binding completely.¹⁴ This mutant was reported to have a very high *in vivo* CL (in rodents and monkey) and a short-terminal elimination half-life.²⁸ In the IgG YTE mutant *M252Y/S254T/T256E*, 3 amino acids were replaced, enabling the IgG to form additional hydrogen bonds with FcRn that enhance binding at pH 6.0 which in monkey and human leads to an increased terminal half-life.¹⁶ In addition, we included a ³H-labeled chicken IgY as a non-binding control.

Human FcRn Transcytosis assay

As depicted in Fig. 3, the paracellular marker showed a negligible flux (P_{app} of 0–2 nm/s) across monolayers of both cell lines, demonstrating the tightness of the cell layer under the applied assay conditions. Chicken IgY and AAA IgG mutant, which do not bind to human FcRn, showed equally low transcytosis values in human FcRn cells. The Wt IgG reached a 2-fold higher flux than the 2 non-binders and the FcRn-binding-enhanced YTE IgG mutant displayed a transcytosis rate of ~20 nm/s. The flux differences of the 3 Fc mutants (AAA vs. Wt vs. YTE) were statistically significant from each other (P value \leq 0.04 in paired t-test).

The transcytosis of all compounds across EV MDCK cells was consistently in the background range and similar to the dextran flux as expected due to the lack of human FcRn expression. Overall, the measured transcytotic flux increased with increasing mAb affinity to the FcRn receptor.

To maximize the resolution of the assay, the effect of different incubation times (3 vs. 5 hrs) and pH gradients (pH 6.0/8.0 vs. pH 6.0/7.4) were assessed with the same Fc mutants and the chicken IgY as a non-binding control (Fig. 4). The pH 6.0/

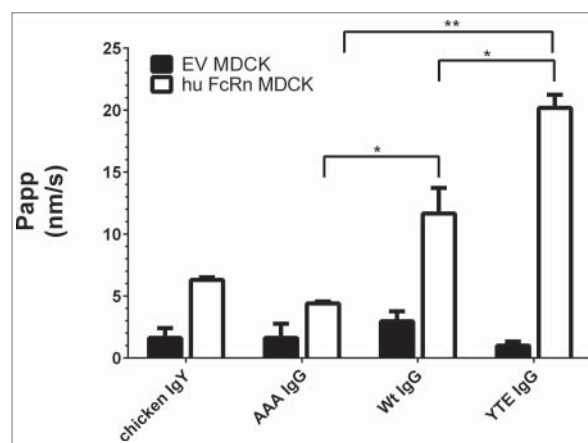


Figure 3. Transcytosis of different ³H-labeled IgG Fc mutants and non-binding control (chicken IgY) at pH 6.0/8.0 in human FcRn MDCK cells and EV MDCK cells as negative control. AAA, Wt, and YTE IgG clearly differed by their flux (Papp). Paired t-test P value (AAA vs. Wt IgG) = 0.024; P value (YTE vs. Wt IgG) = 0.041; P value (AAA vs. YTE IgG) = 0.002; Data is shown as mean \pm SD; n = 3 (separate wells).

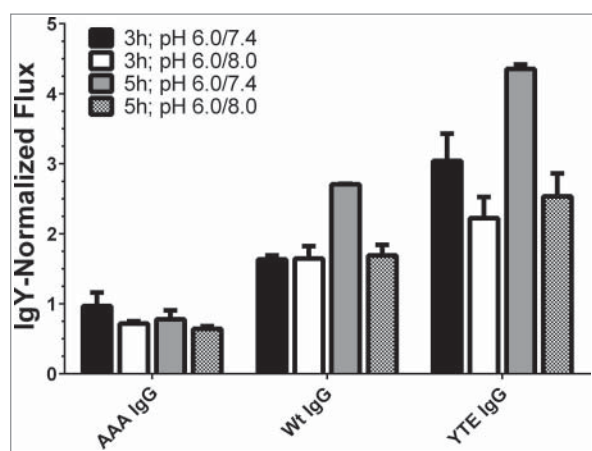


Figure 4. Effect of incubation time and donor/acceptor chamber pH on transcytosis of IgG mutants by human FcRn-over-expressing cells. The application of 5 h incubation time and a pH gradient of 6.0/7.4 differentiated the various molecules best. The fluxes were normalized to the flux of chicken IgY. Data is shown as mean \pm SD; n = 3 (separate wells).

7.4 gradient is more physiologically relevant because the pH of the donor compartment matches that of early endosomes (pH 6.0), while the acceptor compartment pH resembles the blood (pH 7.4). These adjustments led to a better differentiation between the test molecules and the controls. Also, to allow easier comparison among the mAb transcytosis levels within one experiment, transcytosis data in Fig. 4 were reported as “normalized flux” (NF), where the Papp values are divided by the Papp of the chicken IgY, which represent no FcRn-mediated flux and were arbitrarily set to a flux of 1.0.

Rat FcRn Transcytosis assay

The same Fc mutants and control molecules were additionally tested in the same assay set up with rat FcRn-over-expressing MDCK cells. Molecules are often screened in rodents for their PK properties, making the comparison of rat and human FcRn receptors of interest. Table 1 lists the flux values of the different mutants obtained in the rat FcRn system against the results from the human FcRn system (see also Fig. 3). For easier comparison, both data sets were normalized to the respective transcytosis rates of IgY. AAA IgG and IgY had similarly low fluxes across rat and human FcRn MDCK cells, whereas the Wt IgG was transported approximately twice as efficiently. The YTE IgG mutant, however, reached the same transcytosis rate as the Wt IgG in the rat FcRn system, even though in the human FcRn assay the YTE IgG flux markedly exceeded the Wt IgG. Thus, apparently the YTE mutation interacts differently with the FcRn of these 2 species.

Table 1. *In vitro* flux of IgG mutants across human and rat FcRn MDCK cells at pH 6.0/7.4.

Tested antibody	Flux across rat FcRn cells	Flux across human FcRn cells
IgY	1.0 \pm 0.11	1.0 \pm 0.03
AAA IgG	1.34 \pm 0.26	0.70 \pm 0.02
Wt IgG	2.72 \pm 0.31	1.95 \pm 0.12
YTE IgG	2.41 \pm 0.38	3.11 \pm 0.06

Only the YTE mutant showed a species difference in FcRn interaction leading to enhanced flux across human FcRn, but Wt-IgG-like flux across rat FcRn cells. The fluxes were normalized to the IgY flux obtained in the same experiment. Data is shown as mean \pm SD; n = 3 to 6 (separate wells).

In vivo PK evaluation of ^3H -labeled Fc mutants in Wistar rats

To evaluate the relationship between *in vitro* Papp and *in vivo* clearance, the 5 previously introduced ^3H -labeled molecules with different FcRn binding affinities (IgY, anti-Digoxigenin-hu AAA IgG, anti-Digoxigenin-hu IgG Wt IgG and anti-Digoxigenin-hu YTE IgG) were administered as single intravenous dose (i.v.) to male Wistar rats. The plasma concentrations of these molecules were monitored up to 336 or 540 h post dose (Fig. S1 in supplemental material) and their respective PK parameters were determined *via* non-compartmental PK analysis (Table S1 in supplemental material). The plasma exposure of IgY and AAA IgG dropped rapidly after administration, leading to a very high systemic total CL of 36.4 mL/day/kg for the AAA mutant and 52.5 mL/day/kg for the IgY. As expected, the Wt IgG and the YTE IgG showed 6.5-fold and 7.9-fold lower CL than the AAA-IgG, respectively, as a result of the FcRn-mediated protection from mAb degradation *in vivo*. Interestingly, the YTE and Wt IgG showed a very similar PK profile. This confirmed that the YTE mutation does not lead to a half-life-extending effect in rodents, in contrast to the effect seen in monkey or human,¹⁶ and revealed one limitation of the use of rodents as a suitable model to evaluate PK of particular Fc-engineered biologics.

Correlation of antibody FcRn-mediated transcytosis *in vitro* to *in vivo* systemic clearance in rat

To evaluate the *in vivo* relevance of the FcRn transcytosis assay, the flux obtained in rat FcRn-over-expressing cells for the IgY, AAA IgG, wt IgG and YTE IgG was compared with their corresponding systemic clearance derived from single dose PK studies in rats (Table S1 in supplemental material).

As FcRn-mediated Ab binding is *in vivo* a salvage mechanism reducing antibody clearance, higher transcytosis-mediated flux is expected to result in a lower *in vivo* clearance. Indeed, the IVIVC followed an inverse relationship to the *in vitro* flux (Fig. 5). Although the data set is limited, the rat *in*

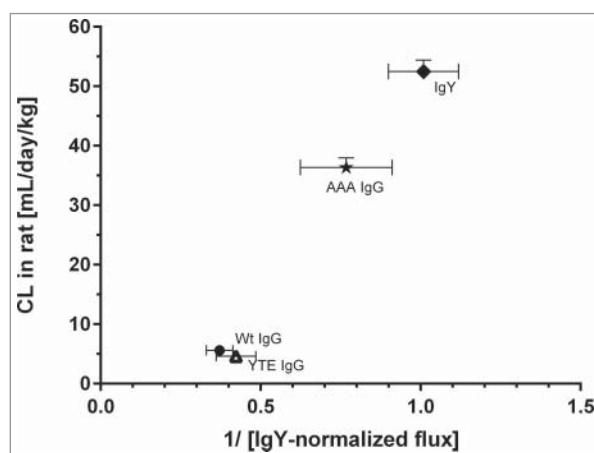


Figure 5. Mean systemic clearance observed in rat after single mAb intravenous administration plotted against the reciprocal normalized flux obtained from the rat FcRn cellular transcytosis assay. IgY-normalized *in vitro* flux of 5 mAbs were inversely proportional with the corresponding *in vivo* CL values in rat. Data is shown as mean \pm SD.

vitro FcRn assay was able to correctly rank mAbs with respect to their FcRn-mediated salvage from degradation *in vivo*.

Correlation of antibody FcRn-mediated transcytosis *in vitro* to *in vivo* systemic clearance in cynomolgus monkeys

Cynomolgus monkey (henceforth referred to as “monkey”) is the most predictive preclinical species for the assessment of mAb PK in human, since monkey FcRn shares a 96% sequence identity (98% homology) with human FcRn.²⁰ Additionally, the effect of Fc engineering on mAb PK in human was described to be well reflected in this species.¹⁷ Therefore, *in vivo* monkey data were used to establish a correlation to *in vitro* human FcRn transcytosis data. The *in vitro* transcytosis data from the human FcRn system was compared with systemic clearance data observed in monkey PK studies performed for 24 mAbs. To avoid contribution of non-FcRn-mediated CL in the IVIVC, such as target-mediated antibody disposition and immunogenicity, only PK studies performed at target-saturating mAb

doses were included and we excluded the data from animals displaying circulating anti-drug antibodies.²⁹

The *in vitro* flux from the human FcRn cellular system and the *in vivo* PK parameters derived in monkey are summarized in Table 2. Flux values were normalized to the Papp value of the wildtype (Wt) <DIG> IgG1 “mAb 2,” the control mAb used in assay validation experiments (Fig. 3 to 5). This enabled a quantitative comparison of Papp values across different experiments reducing potential interference by fluctuation of cellular FcRn expression and functionality.

Fig. 6A depicts the Wt-normalized *in vitro* flux (Wt-NF) of these 24 mAbs across human FcRn-over-expressing MDCK cells plotted against their respective *in vivo* CL in cynomolgus monkeys.

For easier visualization, we plotted the reciprocal Wt-normalized *in vitro* flux (Wt-NF) values across human FcRn-over-expressing MDCK cells against a mAb’s respective *in vivo* CL in cynomolgus monkeys. Fig. 6A only shows the data from mAbs mutated in their FcRn binding region and their corresponding Wt mAbs: AAA IgG No. 1 vs. Wt IgG No. 2 (star), AAA IgG No. 6 vs. Wt IgG No. 5 (cross), FcRn-enhanced IgG

Table 2. Human *in vitro* and cynomolgus monkey *in vivo* data used for the *in vitro-in vivo* correlation

Tested antibody	Description	<i>In vivo</i> data				<i>In vitro</i> data Wt IgG-normalized <i>in vitro</i> flux pH 6.0/7.4
		Dose (mg/kg)	Terminal half life (h)	Total CL (mL/day/kg)	Number of animals	
mAb 1	hu IgG1, AAA mutant; FcRn non-binder	0.3	53	16.1	2	0.31 ± 0.01
mAb 2	hu IgG1, FcRn Wt binder	0.3	79	6.49	2	1.00 ± 0.09
mAb 3	hz IgG1, FcRn Wt binder	10	310 ± 57	3.12 ± 0.55	4	1.64 ± 0.23
mAb 4	hu IgG1, FcRn Wt binder	75	269	5.23	2	0.97 ± 0.07
mAb 5	hu IgG1, FcRn Wt binder	0.3	108	3.84	2	0.63 ± 0.09
mAb 6	hu IgG1, AAA; FcRn non-binder	0.3	32	15.4	2	0.25 ± 0.01
mAb 7	hu IgG1, FcRn Wt binder with FcRn-unrelated CL component	1	178	24.7*	3	0.84 ± 0.1
mAb 8	chimeric IgG (hu Fc), FcRn Wt binder	5	NC*	3.60*	2	0.91 ± 0.1
mAb 9	chimeric IgG (hu Fc), FcRn Wt binder	0.8	380 ± 89	2.46 ± 0.35	3	0.95 ± 0.18
mAb 10	hu IgG1, enhanced FcRn-binding; positive charge patches	20	288	2.86	2	4.14 ± 0.82
mAb 11	hz IgG1, FcRn Wt binder (bevacizumab, Avastin)	5	Deng et al ²⁰	3.97	Deng et al ²⁰	0.83 ± 0.07
mAb 12	hu IgG1, FcRn Wt binder	20	235 ± 156	4.52 ± 1.07	3	1.27 ± 0.1
mAb 13	hu IgG1, enhanced FcRn-binding	20	137 ± 73	3.51 ± 0.8	3	3.42 ± 0.15
mAb 14	hz IgG1, FcRn Wt binder (trastuzumab, Herceptin)	5	Deng et al ²⁰	5.52	Deng et al ²⁰	1.77 ± 0.03
mAb 15	hu IgG4, FcRn Wt binder	2.5	355 ± 34	2.56 ± 0.33	3	1.10 ± 0.2
mAb 16	hu IgG1, FcRn Wt binder	10	59	9.81	2	1.03 ± 0.09
mAb 17	hz IgG1, FcRn Wt binder	10	194	5.88	2	1.06 ± 0.05
mAb 18	hz IgG1, FcRn Wt binder	0.15, 1.5, 15, 150	150*	5.86*	8	1.41 ± 0.06
mAb 19	hu IgG1, FcRn Wt binder	100	282	4.49	2	1.49 ± 0.26
mAb 20	hz IgG1, FcRn Wt binder	50	NC*	3.34*	3	2.13 ± 0.35
mAb 21	hu IgG1, FcRn Wt binder	1	218 ± 74.6	3.74 ± 0.32	4	1.07 ± 0.34
mAb 22	hz IgG1, FcRn Wt binder	30	240	4.61	2	0.95 ± 0.07
mAb 23	hz IgG1, FcRn Wt binder	30	94.2	3.57	2	1.11 ± 0.16
mAb 24	hu IgG1, FcRn Wt binder	150	242	8.16*	6	2.75 ± 0.19

*PK parameters estimated by population approach, no SD applicable mAb systemic clearance from non-compartmental (NCA) PK analysis and terminal half-life after intravenous dose to monkeys is reported together with the respective mAb wt-normalized Papp from human cellular FcRn assay (pH 6.0/7.4). Data are given as mean values ± standard deviation in case of > 2 subjects or measurements.

hu: human; hz: humanized; Wt: wildtype mAb without mutations of the FcRn-binding sites; TMDD: target-mediated drug disposition.

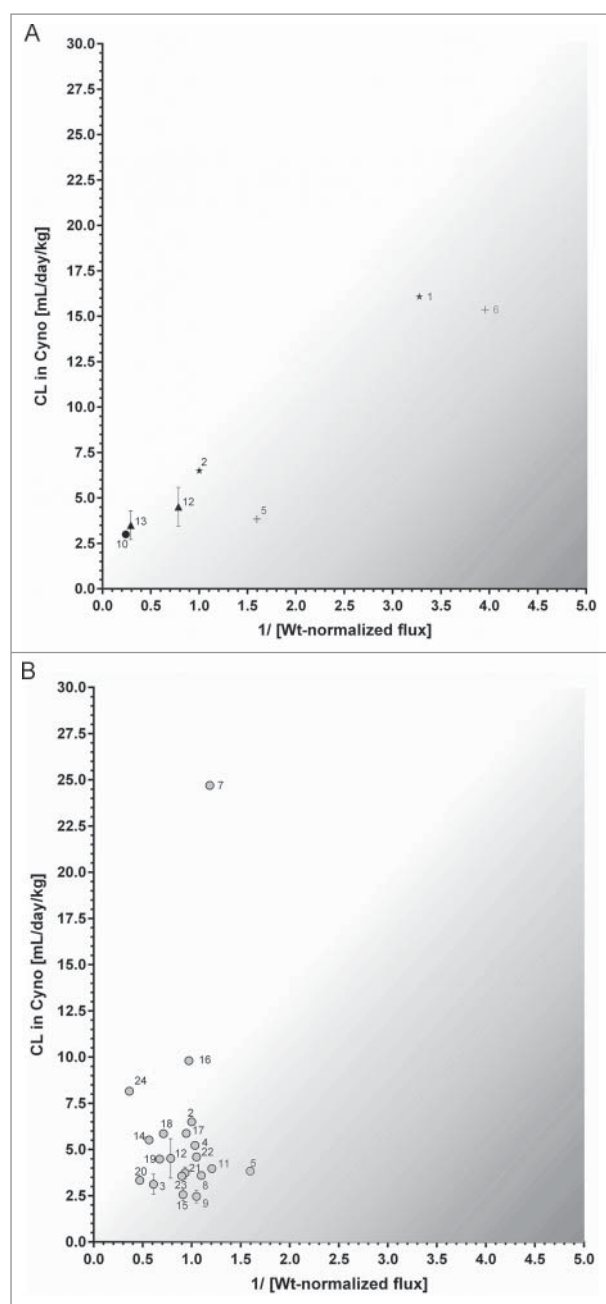


Figure 6. (A) Correlation of reciprocal Wt IgG-normalized *in vitro* flux (pH gradient 6.0/7.4) of 7 mAbs across human FcRn MDCK cells with *in vivo* clearance in cynomolgus monkey. Data is plotted as mean values \pm SD. Corresponding pairs of Fc mutant and Wt IgG are labeled with the same symbol (closed triangle, star, cross). The greyish area roughly indicates mAbs for which *in vivo* CL is hypothesized to be affected by “decelerating” processes, for mAbs in the white area “CL-accelerating” processes are thought to be involved. (B) Correlation of reciprocal Wt IgG-normalized *in vitro* flux (pH gradient 6.0/7.4) of 20 mAbs with wildtype FcRn binding ability across human FcRn MDCK cells with *in vivo* clearance in cynomolgus monkey. Data is plotted as mean values \pm SD for CL and as reciprocal mean values of the Wt IgG-NF. The greyish area roughly indicates mAbs for which *in vivo* CL is hypothesized to be affected by “decelerating” processes, for mAbs in the white area “CL-accelerating” processes are thought to be involved.

No. 13 vs. Wt IgG No. 12 (closed triangle) and the FcRn-enhanced IgG No. 10 (corresponding Wt IgG n.a.). Similar to the rat IVIVC (Fig. 5), the plot revealed an inverse relationship between these 2 parameters.

The 2 AAA-mutated mAbs (mAb 1 and 6) showed a very high systemic CL in monkeys of about 15 mL/day/kg, due to the lack of FcRn-mediated recycling. This also led to

low *in vitro* flux values in FcRn transcytosis assay compared with their respective Wt IgGs.

On the other hand, 2 mAbs with enhanced FcRn affinity (mAbs 10 and 13) both showed low *in vivo* CL of 2.9 (mAb 10) and 3.5 mL/day/kg (mAb 13), as their FcRn-mediated recycling and thus plasma residence time was increased. This consistently translated into enhanced *in vitro* Wt-normalized flux ratios (NF) of 4.1 (mAb 10) and 3.5 (mAb 13) in our cell system.

Most of the tested molecules, however, consisted of Wt-FcRn binders that had different complementarity-determining regions, and thus different molecular properties. Their respective *in vivo* CL values in monkey were very diverse, ranging from 2 to 25 mL/day/kg, which exceeds the range of 2–10 mL/day/kg reported for other FcRn binding competent IgG1s.²⁰ The respective range of *in vitro* Wt-NF flux at pH 6.0/7.4 was 0.6 to 2.8 (Table 2). When plotting these *in vitro* and *in vivo* data (Fig. 6 B), however, no linear correlation could be derived.

Based on these results, the CL of a mAb whose elimination mechanism is mainly FcRn-modulated is likely to follow this inverse relationship with its *in vitro* flux. If CL is dominated by additional “CL-accelerating” factors, mAbs may digress into the upper left part of the 2 IVIVC plots (roughly indicated by the white background area in Fig. 6A and B); in the case of “CL-decelerating” influences, such as low pinocytotic uptake, such mAbs might appear into the lower right part (greyish background area).

Discussion

The PK of mAbs is influenced by many factors, such as the biologic target(s) (including turnover, expression level and tissue distribution), affinity to FcRn receptor, immunogenicity, the presence of off-target binding, catabolism, and mAb physicochemical properties (e.g. isoelectric point and charge patch distribution).^{8,9,30} Several engineered antibodies bearing specific mutations in the FcRn-binding sites have been extensively studied with regards to their ability to prolong residence time in circulation.⁷

Preclinical *in vivo* PK studies are in general of great help for understanding mAb clearance mechanisms, and thus for predicting human PK profiles and identifying possible PK-related liabilities early in drug discovery.²⁰ However, depending on antibody properties/format and intended human dose/administration route, factors like species-specific FcRn receptor and antigen(s) expression/turnover/affinity can remarkably affect mAb PK behavior, and consequently increase challenges and uncertainties in translating the PK profile from animal into human.

To characterize the interplay between various mAb clearance pathways and estimate which of them predominantly drive drug candidate disposition *in vivo*, the availability of *in vitro* tools to study and address in a quantitative manner specific clearance mechanisms may be of great help. Such *in vitro* readouts should support antibody optimization and improve the accuracy of human translations in early in drug discovery. As already established in small molecules drug discovery, *in vitro* screening of PK properties of mAbs can reduce optimization cycles, expand the number of candidates that can be

evaluated, and can be beneficial to “refine,” “reduce” and “replace” animal studies (3Rs).³¹

Here, we characterized and applied a cellular FcRn transcytosis assay using cells expressing either rat or human FcRn receptor (basic assay principle previously introduced by Praetor *et al.*²⁶ and Tesar *et al.*²⁵), to assess mAb *in vitro* transcytosis rate and to use it as an indicator for the FcRn-mediated salvage from intracellular degradation of IgGs, also called “recycling,” known to occur *in vivo*.¹³

The derived *in vitro* transcytotic flux for 4 mAbs in the rat FcRn assay and 24 mAbs in the human FcRn assay was then compared with their *in vivo* clearance (CL) in rat or cynomolgus monkey, respectively, to evaluate whether this *in vitro* readout shows *in vivo* relevance, and consequently whether it could be reliably used in drug discovery projects as a screening and mechanistic tool for mAb candidate optimization and selection.

The cellular FcRn assay was clearly able to differentiate unspecific antibody uptake from FcRn-mediated uptake and transcytosis, as we only detected low background fluxes in “empty vector” MDCK cells lacking human/rat FcRn expression. In addition, mAb flux across human/rat FcRn-overexpressing MDCK cells at pH gradient conditions (pH 6.0/8.0) far exceeded the mAb flux obtained when pH was kept at 8.0 at both sides of the cell layer.

The use of FcRn-overexpressing cells and the application of a pH gradient to induce detectable FcRn-mediated endocytotic uptake followed by transcytosis markedly differs from the process occurring *in vivo*, where mAb endocytotic uptake occurs instead *via* fluid-phase pinocytosis only.

Additionally, both endogenous IgGs and therapeutic mAbs bind to FcRn, and inhibition of FcRn-IgG interactions by administration of very high dose of intravenous immunoglobulins is known to lead to accelerated pathogenic antibody CL *in vivo* and disease amelioration in auto-immune patients.¹⁸ In our FcRn *in vitro* assay, endogenous IgGs were intentionally not included in the donor compartment to ensure maximal dynamic range for the Papp values and allow mechanistic investigations and ranking of FcRn-mediated transcytosis of the studied mAb.

The FcRn transcytosis assay could capture species-specific differences in IgG transcytosis rate, as well as correctly rank wild type *vs.* Fc-mutated mAbs (AAA and YTE) according to their respective observed PK behavior *in vivo*. The different transcytosis rates of the diverse Fc mutants support the requirement of the FcRn receptor for transcellular trafficking of an IgG in the studied cell system, since low / no binding to FcRn receptor led to less transcytosis.

It is well known that human and mouse FcRn have different binding affinities for IgGs from different species. As reported by other authors,^{32,33} human FcRn only binds human, guinea pig and rabbit IgG, whereas mouse FcRn binds IgGs from many different species with high affinity. Human IgG1 binds cynomolgus monkey FcRn with a 2-fold higher affinity than human FcRn, and binds both, mouse and rat FcRn with a 10-fold higher affinity than human FcRn.¹⁵

In this work, for the YTE mutant, species-selective differences in rat and human FcRn IgG interactions were observed. This is probably related to differences in mAb pH-dependent binding properties for the 2 FcRn receptor homologues, and

thus different binding/release behavior at endosomal and blood pH, respectively. Theoretically, an increased FcRn receptor binding affinity of a mAb at pH 6.0, as reported for the YTE mutant, should help the recycling of the mAb and thus reduce its clearance *in vivo*.¹⁶ However, as also described by Vaccaro *et al.* for a different Fc mutation,³⁴ the YTE mutant might also possess enhanced binding affinity to murine FcRn at pH 7.4, resulting in a reduced release of the IgG to the blood stream and thus increased cellular degradation. Conversely, the binding of the YTE mAb to the human FcRn at pH 7.4 was low, resulting in an increased *in vitro* flux in the human FcRn cellular system, exceeding that of the wt-IgG. This indicates that the studied assay not only identifies differences in FcRn affinity at pH 6.0 across animal species, but can help to reveal the overall effect of the mutations on the various processes, including receptor binding, FcRn-IgG-complex trafficking and IgG release.

Given the additive nature of mAb systemic clearance process,⁹ expected to occur also for large molecules, and the lack of target antigen expression in our cellular system, a direct correlation between *in vitro* transcytotic flux and *in vivo* CL can be expected only for biologics whose clearance mechanism at the studied dose levels is modulated predominantly by its interactions with the FcRn receptor, and not in cases where CL is affected by other processes, such as the formation of anti-drug antibodies or other immunogenic reactions, by TMDD when non-saturating drug doses are studied, by specific sequence instability and catabolism, or by an enhanced non-specific cellular pinocytotic uptake.³⁵

The rat FcRn *in vitro* flux to *in vivo* rat CL correlation shown here indicated an inverse relationship of the 2 parameters. When comparing the human FcRn *in vitro* flux to the observed *in vivo* CL in cynomolgus monkeys, again the AAA mutants with high CL displayed a low *in vitro* flux, whereas mAbs with enhanced FcRn affinity and consequently low CL showed a stronger transcytosis in the cellular assay. The Wt-FcRn binders with CL values from 2 to 25 mL/day/kg showed an *in vitro* “Wt IgG-normalized flux” (NF) range from 0.6 to 2.8. Therefore, mAbs within this range could be considered to have “normal” FcRn interaction properties. For this mAb cluster, no obvious quantitative correlation between the *in vivo* CL and the FcRn-mediated flux *in vitro* was observed, despite the absence of TMDD at the tested dose levels and immunogenicity *in vivo*.

The fact that mAbs with very similar *in vitro* flux, still showed considerable differences in *in vivo* CL could be explained by additional CL processes, apart from FcRn recycling, not present in the cellular assay. One example is mAb 7, which showed an extremely high systemic CL in monkey (25 mL/day/kg) even though it had a non-mutated Fc scaffold and its *in vitro* flux was similar to a mAb with normal *in vivo* CL < 10 mL/day/kg.²⁰ The more mAbs digress from a linear relationship between *in vitro* FcRn-mediated transcytosis and *in vivo* CL, the more their PK is expected to be affected by additional “CL-accelerating” processes, such as enhanced pinocytosis or off-target binding, or “decelerating” processes, such as low unspecific uptake.

It should be noted that, in contrast to the PK data available for rat where most mAbs shared the same Fab structure and epitope (anti-DIG) and were evaluated in the same *in vivo*

experiment, the clearance data set used for the human FcRn flux/monkey CL-IVIVC were obtained at different dose levels, with different study designs and bioanalytical assays, and using different monkey colonies (thus animals of various ages/origins), which can increase data variability and reduce the accuracy of the IVIV correlation. In addition, the mAbs tested in monkey PK studies have different scaffolds and are not directed against the same target epitope, resulting in large differences in physicochemical properties and 3D structures, whose effect on FcRn-mediated recycling and cellular trafficking occurring *in vivo* might not be captured in this cellular system. Additionally, cynomolgus monkey and human FcRn receptor sequence/expression are very similar but not entirely identical.²⁰ To further evaluate this aspect and to calibrate the IVIVC with clinical data, we are currently selecting more mAbs for *in vitro* testing for which systemic clearance in man is available from Roche clinical trials or reported in literature. For mAbs with monkey PK that does not translate well into man due to species-dependent FcRn differences, the IVIVC is expected to improve. However, the correlation could also get worse if additional FcRn-unrelated clearance processes take place in man which are absent in monkey, such as a human-specific off-target binding.

After intracellular uptake *in vivo*, an antibody can either enter the “recycling pathway” occurring *via* FcRn-receptor interactions, or the “degradative (lysosomal) pathway.”³⁶ This is dependent on the degree of interaction with the FcRn receptor and the level of occupancy of the FcRn receptors in the endosomes, which is a saturable process.

In vitro, due to the high expression level of FcRn in the transfected MDCK cells we used, which is much higher than under physiologic conditions, it is likely that most/all of the IgG molecules internalized under pH gradient conditions at pH 6.0/7.4 are further trafficked intracellularly by FcRn and no saturation occurs. At the same time, an unspecific cellular uptake of a mAb, which might be enhanced by certain physicochemical properties, e.g., large positive charge patches, can also occur under pH gradient conditions and contribute to the flux measured in this work at pH 6.0/7.4. It should be noted that an antibody molecule showing a high degree of unspecific cellular uptake (i.e., non-target- and non FcRn-mediated) occurring *via* fluid-phase pinocytosis is expected to be more prone to undergo intracellular degradation. Indeed, a higher fraction of the total antibody amount is internalized independently of its binding to FcRn and is thus not protected by lysosomal degradation.⁸ Therefore, increased unspecific cellular uptake of a mAb might counteract the prolongation of *in vivo* residence time expected by an increased FcRn binding affinity.³⁷

These considerations are well in line with the observations for mAb 10, which was specifically designed to display enhanced FcRn affinity and a certain positive charge patch distribution to increase pinocytotic cellular uptake.^{8,38} This combination resulted in increased flux in the transcytosis assay, but a residence time in monkeys comparable to non-mutated IgG₁, as pinocytosis and FcRn-mediated effects highly likely compensate each other *in vivo*.

This counter-activity of pinocytosis and FcRn-mediated salvage *in vivo* is also the reason why we chose the pH gradient conditions for the IVIVC. When applying pH 7.4 in both

chambers, mAb uptake will solely happen *via* pinocytosis. Thus, we can assume that a mAb with high FcRn affinity, but low pinocytotic uptake, would reach a similar or even lower transcytotic flux than a mAb with average FcRn affinity and high pinocytotic uptake. As described above, a mAb with high pinocytotic uptake behavior undergoes a more rapid clearance as opposed to a mAb with low non-specific cellular uptake potential. Thus, the pinocytotic uptake component is considered to be a confounding element for our *in vitro* readout, where an enhanced transcytotic flux is in general interpreted as a hint for low *in vivo* CL due to proper FcRn salvage.

In summary, our cellular FcRn assay was able to detect and quantitatively measure the FcRn-mediated transcytosis occurring *in vitro* for various therapeutic IgGs. Beside describing further validation of the *in vitro* FcRn assays initially reported by Praetor²⁶ and Tesar,²⁵ this work evaluates for the first time the correlation between *in vitro* transcytosis and *in vivo* preclinical PK data for 25 antibody-based molecules. Despite the discussed limitations and need for further mechanistic investigations before quantitatively using the *in vitro* flux for, for example, physiologically based PK modeling purposes, this cellular assay looks promising for a first *in vitro* evaluation of potential liabilities in antibody FcRn-mediated clearance, with the aim to rank candidates and reduce the number of molecules tested *in vivo*. Although it does not cover all the biologic processes involved in mAb recycling and degradation *in vivo*, it helps to understand the contribution of the FcRn-mediated recycling to mAb PK and highlights that mAb disposition *in vivo* is a phenomenon likely more complex and more peculiar for each antibody than has been considered so far.

Material and methods

Antibodies

Fluorescein isothiocyanate (FITC)-labeled antibodies (rat IgG, mouse IgG and chicken IgY) were purchased from Jackson ImmunoResearch (Cat.No. 012-090-003, 015-090-003 and 003-090-003, respectively), FITC-human IgG from Sigma-Aldrich (Cat.No. F 9636). The paracellular marker FITC-dextran (150 kDa) was obtained from Sigma-Aldrich. Chimeric, human or humanized unlabeled antibodies with/without Fc mutations were generated at Hoffmann- La Roche as part of various discovery and development projects; due to company policy on chemical name disclosure, structures and targets for Roche mAbs are not reported here. Fc mutants were designed in a way to specifically alter the FcRn-binding affinity of the molecule. All other antibodies were considered as «wildtype» FcRn-binders. All tested unlabeled mAbs are listed in Table 2.

³H-labeling of antibodies

Five molecules (anti-Digoxigenin-YTE (M252Y/S254T/T256E) IgG; anti-Digoxigenin AAA (M252A/H310A/H435A) IgG; anti-Digoxigenin Wildtype IgG; chicken IgY; human Wt IgG Fc fragment) were ³H-labeled according to the following protocol in a representative example. Chicken IgY was purchased from Jackson ImmunoResearch, the anti-DIG IgGs had been generated internally.

Four mg (0.0274 μmol) of antibody in 377 μL formulation buffer (20 mM His, 140 mM NaCl, pH 6) was diluted with 100 μL labeling buffer (DPBS pH 8.5, pH was adjusted with 1 N aq. NaOH) and placed into a 3500 MWCO Midi D-TubeTM Dialyzer. The solution was dialyzed against labeling buffer; the buffer was changed 3 times each after 45 minutes and stored in the refrigerator overnight. 13.1 μg (6.6 mCi, 0.074 μmol) of [³H]-N-succinimidyl propionate (NSP) was transferred into a 1.5 mL Eppendorf LoBind tube and dissolved in 15 μL dimethylsulfoxide. Antibody solution was added to the Eppendorf vial and the solution was shaken for 15 minutes at room temperature. After this time, 1 μL of 1 M lysine, dissolved in labeling buffer, was added to stop the reaction. The reaction solution was transferred into a 3500 MWCO Midi D-TubeTM Dialyzer and dialyzed against the formulation buffer. The buffer was changed 3 times each after 45 minutes and stored in the fridge overnight. The protein concentration was determined by UV at 280 nm (Eppendorf BioSpectrometer). The radioactivity was determined by liquid scintillation counting (Hidex 300SL and ULTIMA GOLDTM cocktail). Specific activities were achieved in the range of 900 $\mu\text{Ci}/\text{mg}$ to 1200 $\mu\text{Ci}/\text{mg}$. The radiochemical purity of > 95% was determined by size-exclusion chromatography.

Cell culture

MDCK cells transfected with rat FcRn and rat $\beta_2\text{m}$ were kindly provided by Prof. Pamela Bjorkman (CalTech, Los Angeles, US) and were maintained according to Tesar *et al.*²⁵ in SMEM (Gibco, Life Technologies), supplemented with 10% fetal bovine serum (FBS, Sigma-Aldrich), 10'000 IU/ $\mu\text{g}/\text{mL}$ penicillin-streptomycin (Gibco, Life Technologies), 2mM L-Glutamine (Gibco, Life Technologies) and 0.2 mg/mL geneticin (Gibco, Life Technologies) at 37°C, 5% CO₂. MDCK cells transfected with human FcRn and empty vector (EV) were kindly provided by Prof. Walter Hunziker, (Singapore University) and were maintained according to Praetor *et al.* in DMEM (Gibco, Life Technologies), supplemented with 10% FBS (Sigma-Aldrich), 10'000 IU/ $\mu\text{g}/\text{mL}$ penicillin-streptomycin, 20 mM HEPES (Gibco, Life Technologies) and 0.5 mg/mL geneticin at 37°C, 5% CO₂. All the cells were passaged twice per week.

For experiments requiring polarized cell monolayers, cells were seeded at superconfluent density (0.25×10^6 cells/mL) onto 6.5 mm diameter 24-well Transwell[®] polycarbonate filters, 0.4 μm pore size (Corning Costar), with 0.3 and 1.0 mL of media in the apical and basolateral reservoirs, respectively. In the Transwell[®] system, rat FcRn MDCK cells were maintained in MEM (Sigma-Aldrich) supplemented with 10% FBS, 10'000 IU/ $\mu\text{g}/\text{mL}$ penicillin-streptomycin and 0.2 mg/mL geneticin at 37°C, 5% CO₂, were fed on day 3 after initial seeding and used for experiments on the fourth day post plating. Human FcRn and EV MDCK cells were maintained in the same medium and conditions as in the flask were fed the second or third day after initial seeding and used for experiments on the third or fourth day post plating, respectively.

Prior to incubations with the test compounds, the designated receiver plate was blocked for 24 h with 1% bovine serum albumin (BSA) at 4°C to prevent mAb adsorption to the plate surface. Cells were serum-starved for 2 to 2.5 h in their

respective medium without FBS, washed once with HEPES (Sigma-Aldrich)-buffered Hanks' balanced salt solution with Ca²⁺ and Mg²⁺ (HBSS++; Gibco, Life Technologies) pH 7.4 and finally pre-incubated for 30 minutes with MES (Sigma-Aldrich)-buffered HBSS++ pH 6.0 (donor compartment) or HEPES-HBSS++ pH 7.4 (acceptor compartment) or with HEPES-HBSS++ pH 7.4 in both compartments as a control.

Quantitative transcytosis assay

Test antibody (³H-labeled, fluorescently labeled or unlabeled) was added at the indicated final concentration in HBSS++ pH 6.0, pH 7.4 or 8.0 (the 2 latter for control experiments) and 0.1% BSA in 0.6 mL in the basolateral chamber, which served as donor compartment. The apical chamber was filled with 0.2 mL of HBSS++ pH 7.4 or pH 8.0 containing as well 0.1% BSA. FITC-dextran (150 kDa) at 100 nM was incubated as paracellular marker in separate wells for each experiment. Plates were then incubated at 37°C or 4°C (for control measurements), 5% CO₂, for the indicated durations. At the end of the experiment, samples were taken from the acceptor and donor compartment and for ³H-labeled compounds, concentration was measured *via* liquid-scintillation counting (LSC) in Luma-Plate-96, White Opaque Microplate with Scintillate Coated on the Bottom (Perkin Elmer) in a Top Count Plate reader NXT (HTS) on the following day. Fluorescently labeled molecules were measured in 384-wells black plate (Greiner) in a Multi-plate reader system for fluorescence (Perkin Elmer) and concentration calculation was based on calibration curves for each compound in the given buffer system. Unlabeled human IgGs were analyzed by quantitative ELISA.

ELISA (enzyme-linked immunosorbent assay)

Concentrations of unlabeled human(ized) IgGs were determined by appropriate enzyme-linked immunoassays. Anti-human-IgG, Fc γ -specific and Anti-human F(ab)₂-F(AB₂)-Biotin (Jackson ImmunoResearch), were used for capturing and detection, respectively, in combination with Poly-HRP40-Streptavidin (Fitzgerald) and Supersignal chemiluminescent (Thermo scientific). PBS +0.1% Tween 20[®] was used as wash buffer and PBS +0.5%BSA +0.05% Tween 20[®] was used as blocking and assay buffer. All washing steps were performed in the Biotek ELx405 washer: 4 times after blocking and incubation with the samples, and 6 times after incubation with the detection Ab and the HRP-conjugate. All incubation steps with exception of the coating period (4°C overnight, no shaking) were performed at room temperature (RT) with shaking at 450 RPM.

ELISA plates (Nunc ImmunoMaxiSorp) were coated with 0.1 $\mu\text{g}/\text{mL}$ of capturing antibody in PBS followed by at least 1 hour of blocking. Then, serially diluted assay samples (1:8, 1:32 and 1:128) and a calibration curve (range detection: 34 pg/mL –25 ng/mL) for each test compound prepared in assay buffer were added and incubated for 1.5 to 2 hours. Subsequently, bound test IgG was detected by incubating with 50 ng/mL of detection antibody for 1.5 to 2 hours, followed by incubation with 1 ng/mL of HRP-conjugate for 20 to maximally 30 minutes. Finally, the chemiluminescence substrate was

added and the signal was measured in the Multiplate reader system for luminescence (Perkin Elmer). The data was processed with SoftMax Pro Data Acquisition and Analysis Software (Molecular Devices).

Single-dose Pharmacokinetic Studies with ^3H -antibodies in rats

Adult male Wistar rats weighing ~ 250 g were obtained from Harlan Laboratories (Horst, Netherlands) and housed at F. Hoffmann La-Roche, Basel, in a controlled environment (temperature, humidity, and 12 h light/dark cycle) with ad libitum access to food and water. All rodent studies were conducted with the approval of the local veterinary authority in strict adherence to the Swiss federal regulations on animal protection and to the rules of the Association for Assessment and Accreditation of Laboratory Animal Care International. The tested antibodies were the following: chicken IgY, anti-Digoxigenin-hu IgG-AAA mutation (AAA IgG), anti-Digoxigenin-hu Wt IgG (Wt IgG); anti-Digoxigenin-hu IgG-YTE mutation (YTE IgG).¹⁶ All molecules were administered in their ^3H -labeled form.

Four rats per compound received $30 \mu\text{Ci } ^3\text{H}$ -antibody in $500 \mu\text{L}$ histidine buffer (20 mM histidine, 140 mM NaCl, pH 6) by i.v. tail vein injection.

Blood samples were collected from the tail vein under mild isoflurane anesthesia into K_2EDTA coated polypropylene tubes at 0.83, 1, 3, 7, 24, 48, 72, 96, 168, 240, 336, 408, 504, 576, 672, 744, and 840 hours after administration. Plasma was prepared within 30 min by centrifugation at 3000 g for 5 min at 4°C and frozen immediately. Then $10 \mu\text{L}$ of plasma and 3.5 mL of Ultima Gold[®] (Perkin-Elmer) were then mixed in 6 mL polyethylene tubes (Perkin Elmer) and the radioactivity counts were measured by a liquid scintillation analyzer (Tri-Carb 3100 TR, Packard Instruments).

Single-dose Pharmacokinetic Studies with cold antibodies in monkeys

Adult cynomolgus monkeys were used for the PK studies. All monkey studies were approved by the Roche Ethical Committee on Animal Welfare and conducted with the approval of the local veterinary authorities and conducted at Roche Innovation Center Basel or at audited Contract Research Organizations. Most of the tested antibodies originated from various internal Roche R&D projects; due to company policy on chemical name disclosure, structures and targets for 22 Roche mAbs are not reported here. The tested compounds were administered as single i.v. injection and the antibody concentrations in plasma or serum were determined by ELISA methodologies. Details of the individual studies are reported in Table 2.

Data analysis

In vitro data was evaluated with Microsoft Excel 2010 (Microsoft). Plotting was performed with Microsoft Excel 2010 and GraphPad Prism 6. Analysis of *in vivo* PK data was performed with Phoenix WinNonlin by NCA (Certara).

Disclosure of potential conflicts of interest

All authors are current or former employees of Roche, Pharmaceutical Research and Early Development, and hold a financial interest in Roche.

Acknowledgments

We thank Maria Stella Gruyer, Peter Schrag, and Claudia Senn for conducting part of the rat and cynomolgus monkey PK studies and Eginhard Schick for his support with the ELISA method establishment (all from Pharmaceutical Sciences, Pharma Research and Early Development, Roche Innovation Center Basel). Moreover, we would like to thank Hubert Kettenberger, Alexander Haas, Mathias Mueller, Dieter Muri, Thomas Hartung, Eike Hoffmann, Erwin van Prukenbrook, Tilman Schlothauer, Jens Fischer, Silke Metz, Marcus Schmid, and Jens Niewoehner from the TMO Department, Roche Innovation Center Basel, Zurich, and Munich for their advices, for the QC of ^3H -labeled mAbs, and for the supply of the mAbs for the IVIVC. We are also grateful to Kevin Brady, Matthias Fueth, Martin Lechmann, Niels Janssen, Wolfgang Richter, Hans-Peter Grimm, Antje-Christine Walz, Erich Koller, and Cristina Bertinetti-Lapatki from Pharmaceutical Sciences, Roche Innovation Center Basel, for the mAb supply, cell characterization, monkey PK data and valuable scientific discussions. Finally, we acknowledge CalTech, Singapore University, for providing the cells and Prof. Dr. Oliver Muehleemann from the University of Bern.

ORCID

Sherri Dudal  <http://orcid.org/0000-0003-2566-8755>

Marie-Elise Brun  <http://orcid.org/0000-0003-1839-0556>

References

- Igawa T, Tsunoda H, Kuramochi T, Sampei Z, Ishii S, Hattori K. Engineering the variable region of therapeutic IgG antibodies. *Mabs-Austin* 2011; 3:243-52; PMID:21406966; <https://doi.org/10.4161/mabs.3.3.15234>
- Klein C, Schaefer W, Regula JT. The use of CrossMab technology for the generation of bi- and multispecific antibodies. *Mabs-Austin* 2016; 8:1010-20; PMID:27285945; <https://doi.org/10.1080/19420862.2016.1197457>
- Nelson AL. Antibody fragments Hope and hype. *Mabs-Austin* 2010; 2:77-83; PMID:20093855; <https://doi.org/10.4161/mabs.2.1.10786>
- Kontermann RE. Half-life extended biotherapeutics. *Expert Opin Biol Ther* 2016; 16:903-15; PMID:26967759; <https://doi.org/10.1517/14712598.2016.1165661>
- Ayyar BV, Arora S, O'Kennedy R. Coming-of-Age of Antibodies in Cancer Therapeutics. *Trends Pharmacol Sci* 2016; 37:1009-28; PMID:27745709; <https://doi.org/10.1016/j.tips.2016.09.005>
- Beck A, Wurch T, Bailly C, Corvaia N. Strategies and challenges for the next generation of therapeutic antibodies. *Nat Rev Immunol* 2010; 10:345-52; PMID:20414207; <https://doi.org/10.1038/nri2747>
- Mimoto F, Kuramochi T, Katada H, Igawa T, Hattori K. Fc engineering to improve the function of therapeutic antibodies. *Curr Pharm Biotechnol* 2016; 17:1298-1314; PMID:27552846; <https://doi.org/10.2174/1389201017666160824161854>
- Li B, Tesar D, Boswell CA, Cahaya HS, Wong A, Zhang JH, Meng YG, Eigenbrot C, Pantua H, Diao JY, et al. Framework selection can influence pharmacokinetics of a humanized therapeutic antibody through differences in molecule charge. *Mabs-Austin* 2014; 6:1255-64; PMID:25517310; <https://doi.org/10.4161/mabs.29809>
- Datta-Mannan A, Lu JR, Witcher DR, Leung D, Tang Y, Wroblewski VJ. The interplay of non-specific binding, target-mediated clearance and FcRn interactions on the pharmacokinetics of humanized antibodies. *Mabs-Austin* 2015; 7:1084-93; PMID:26337808; <https://doi.org/10.1080/19420862.2015.1075109>
- Leavy O. Therapeutic antibodies: past, present and future. *Nat Rev Immunol* 2010; 10:297; PMID:20422787; <https://doi.org/10.1038/nri2763>

11. Sand KMK, Bern M, Nilsen J, Noordzij HT, Sandlie I, Andersen JT. Unraveling the interaction between FcRn and albumin: opportunities for design of albumin-based therapeutics. *Front Immunol* 2015; 5:1-21; PMID:25674083; <https://doi.org/10.3389/fimmu.2014.00682>
12. Martins JP, Kennedy PJ, Santos HA, Barrias C, Sarmiento B. A comprehensive review of the neonatal Fc receptor and its application in drug delivery. *Pharmacol Therapeut* 2016; 161:22-39; PMID:27016466; <https://doi.org/10.1016/j.pharmthera.2016.03.007>
13. Giragossian C, Clark T, Piche-Nicholas N, Bowman CJ. Neonatal Fc receptor and its role in the absorption, distribution, metabolism and excretion of immunoglobulin G-Based biotherapeutics. *Curr Drug Metab* 2013; 14:764-90; PMID:23952252; <https://doi.org/10.2174/13892002113149990099>
14. Schlothauer T, Rueger P, Stracke JO, Hertenberger H, Fingas F, Kling L, Emrich T, Drabner G, Seeber S, Auer J, et al. Analytical FcRn affinity chromatography for functional characterization of monoclonal antibodies. *Mabs-Austin* 2013; 5:576-86; PMID:23765230; <https://doi.org/10.4161/mabs.24981>
15. Abdiche YN, Yeung YA, Chaparro-Riggers J, Barman I, Strop P, Chin SM, Pham A, Bolton G, McDonough D, Lindquist K, et al. The neonatal Fc receptor (FcRn) binds independently to both sites of the IgG homodimer with identical affinity. *Mabs-Austin* 2015; 7:331-43; PMID:25658443; <https://doi.org/10.1080/19420862.2015.1008353>
16. Robbie GJ, Criste R, Dall'Acqua WF, Jensen K, Patel NK, Lososky GA, Griffin MP. A novel investigational Fc-Modified humanized monoclonal antibody, motavizumab-YTE, has an extended Half-Life in healthy adults. *Antimicrob Agents Ch* 2013; 57:6147-53; PMID:24080653; <https://doi.org/10.1128/AAC.01285-13>
17. Dall'Acqua WF, Kiener PA, Wu HR. Properties of human IgG1s engineered for enhanced binding to the neonatal Fc receptor (FcRn). *J Biol Chem* 2006; 281:23514-24; PMID:16793771; <https://doi.org/10.1074/jbc.M604292200>
18. Kuo TT, Aveson VG. Neonatal Fc receptor and IgG-based therapeutics. *Mabs-Austin* 2011; 3:422-30; PMID:22048693; <https://doi.org/10.4161/mabs.3.5.16983>
19. Souders CA, Nelson SC, Wang Y, Crowley AR, Klempner MS, Thomas W, Jr. A novel *in vitro* assay to predict neonatal Fc receptor-mediated human IgG half-life. *mAbs* 2015; 7:912-21; PMID:26018774; <https://doi.org/10.1080/19420862.2015.1054585>
20. Deng R, Iyer S, Theil FP, Mortensen DL, Fielder PJ, Prabhu S. Projecting human pharmacokinetics of therapeutic antibodies from nonclinical data What have we learned? *Mabs-Austin* 2011; 3:61-6; PMID:20962582; <https://doi.org/10.4161/mabs.3.1.13799>
21. Dong JQ, Salinger DH, Endres CJ, Gibbs JP, Hsu CP, Stouch BJ, Hurh E, Gibbs MA. Quantitative prediction of human pharmacokinetics for monoclonal antibodies retrospective analysis of monkey as a single species for First-in-Human prediction. *Clin Pharmacokinet* 2011; 50:131-42; PMID:21241072; <https://doi.org/10.2165/11537430-000000000-00000>
22. Datta-Mannan A, Chow CK, Dickinson C, Driver D, Lu JR, Witcher DR, Wroblewski VJ. FcRn Affinity-Pharmacokinetic relationship of five human IgG4 antibodies engineered for improved *in vitro* FcRn binding properties in cynomolgus monkeys. *Drug Metab Dispos* 2012; 40:1545-55; PMID:22584253; <https://doi.org/10.1124/dmd.112.045864>
23. Gurbaxani B, Dela Cruz LL, Chintalacheruvu K, Morrison SL. Analysis of a family of antibodies with different half-lives in mice fails to find a correlation between affinity for FcRn and serum half-life. *Mol Immunol* 2006; 43:1462-73; PMID:16139891; <https://doi.org/10.1016/j.molimm.2005.07.032>
24. Datta-Mannan A, Chow CK, Dickinson C, Driver D, Lu J, Witcher DR, Wroblewski VJ. FcRn affinity-pharmacokinetic relationship of five human IgG4 antibodies engineered for improved *in vitro* FcRn binding properties in cynomolgus monkeys. *Drug Metab Dispos* 2012; 40:1545-55; PMID:22584253; <https://doi.org/10.1124/dmd.112.045864>
25. Tesar DB, Tiangco NE, Bjorkman PJ. Ligand valency affects transcytosis, recycling and intracellular trafficking mediated by the neonatal Fc receptor. *Traffic* 2006; 7:1127-42; PMID:17004319; <https://doi.org/10.1111/j.1600-0854.2006.00457.x>
26. Praetor A, Ellinger I, Hunziker W. Intracellular traffic of the MHC class I-like IgG Fc receptor, FcRn, expressed in epithelial MDCK cells. *J Cell Sci* 1999; 112:2291-9; PMID:10381385.
27. Ober RJ, Radu CG, Ghetie V, Ward ES. Differences in promiscuity for antibody-FcRn interactions across species: implications for therapeutic antibodies. *Int Immunol* 2001; 13:1551-9; PMID:11717196; <https://doi.org/10.1093/intimm/13.12.1551>
28. Martin WL, West AP, Jr., Gan L, Bjorkman PJ. Crystal structure at 2.8 Å of an FcRn/heterodimeric Fc complex: mechanism of pH-dependent binding. *Mol Cell* 2001; 7:867-77; PMID:11336709; [https://doi.org/10.1016/S1097-2765\(01\)00230-1](https://doi.org/10.1016/S1097-2765(01)00230-1)
29. Chirmule N, Jawa V, Meibohm B. Immunogenicity to therapeutic proteins: Impact on PK/PD and efficacy. *Aaps J* 2012; 14:296-302; PMID:22407289; <https://doi.org/10.1208/s12248-012-9340-y>
30. Hotzel I, Theil FP, Bernstein LJ, Prabhu S, Deng R, Quintana L, Lutman J, Sibia R, Chan P, Bumbaca D, et al. A strategy for risk mitigation of antibodies with fast clearance. *Mabs-Austin* 2012; 4:753-60; PMID:23778268; <https://doi.org/10.4161/mabs.22189>
31. Russell WM. The development of the three Rs concept. *Altern Lab Anim* 1995; 23:298-304; PMID:11656565.
32. Roopenian DC, Akilesh S. FcRn: the neonatal Fc receptor comes of age. *Nat Rev Immunol* 2007; 7:715-25; PMID:17703228; <https://doi.org/10.1038/nri2155>
33. Ober RJ, Radu CG, Ghetie V, Ward ES. Differences in promiscuity for antibody-FcRn interactions across species: Implications for therapeutic antibodies. *Int Immunol* 2001; 13:1551-9; PMID:11717196; <https://doi.org/10.1093/intimm/13.12.1551>
34. Vaccaro C, Bawdon R, Wanjie S, Ober RJ, Ward ES. Divergent activities of an engineered antibody in murine and human systems have implications for therapeutic antibodies. *P Natl Acad Sci USA* 2006; 103:18709-14; PMID:17116867; <https://doi.org/10.1073/pnas.0606304103>
35. Datta-Mannan A, Lu J, Witcher DR, Leung D, Tang Y, Wroblewski VJ. The interplay of non-specific binding, target-mediated clearance and FcRn interactions on the pharmacokinetics of humanized antibodies. *mAbs* 2015; 7:1084-93; PMID:26337808; <https://doi.org/10.1080/19420862.2015.1075109>
36. Grevys A, Bern M, Foss S, Brodie DB, Moen A, Gunnarsen KS, Aase A, Michaelsen TE, Sandlie I, Andersen JT. Fc Engineering of Human IgG1 for Altered Binding to the Neonatal Fc Receptor Affects Fc Effector Functions. *J Immunol* 2015; 194:5497-508; PMID:25904551; <https://doi.org/10.4049/jimmunol.1401218>
37. Datta-Mannan A, Thangaraju A, Leung D, Tang Y, Witcher DR, Lu J, Wroblewski VJ. Balancing charge in the complementarity-determining regions of humanized mAbs without affecting pI reduces non-specific binding and improves the pharmacokinetics. *mAbs* 2015; 7:483-93; PMID:25695748; <https://doi.org/10.1080/19420862.2015.1016696>
38. Igawa T, Tsunoda H, Tachibana T, Maeda A, Mimoto F, Moriyama C, Nanami M, Sekimori Y, Nabuchi Y, Aso Y, et al. Reduced elimination of IgG antibodies by engineering the variable region. *Protein Eng Des Sel* 2010; 23:385-92; PMID:20159773; <https://doi.org/10.1093/protein/gzq009>